

1 Phables: from fragmented assemblies to 2 high-quality bacteriophage genomes

3 Vijini Mallawaarachchi¹, Michael J. Roach¹, Przemyslaw Decewicz^{2,1}, Bhavya
4 Papudeshi¹, Sarah K. Giles¹, Susanna R. Grigson¹, George Bouras³, Ryan D. Hesse¹,
5 Laura K. Inglis¹, Abbey L. K. Hutton¹, Elizabeth A. Dinsdale¹ and Robert A. Edwards¹

6 ¹Flinders Accelerator for Microbiome Exploration, College of Science and Engineering,
7 Flinders University, Bedford Park, Adelaide, SA, 5042, Australia

8 ²Department of Environmental Microbiology and Biotechnology, Institute of
9 Microbiology, Faculty of Biology, University of Warsaw, Warsaw 02-096, Poland

10 ³Adelaide Medical School, The University of Adelaide, North Tce, Adelaide, SA, 5000,
11 Australia

12

13 Keywords: bacteriophages, metagenomics, genomics, assembly graphs

14 Abstract

15 Motivation

16 Microbial communities influence both human health and different environments. Viruses
17 infecting bacteria, known as bacteriophages or phages, play a key role in modulating bacterial
18 communities within environments. High-quality phage genome sequences are essential for
19 advancing our understanding of phage biology, enabling comparative genomics studies, and
20 developing phage-based diagnostic tools. Most available viral identification tools consider
21 individual sequences to determine whether they are of viral origin. As a result of the challenges
22 in viral assembly, fragmentation of genomes can occur, leading to the need for new approaches
23 in viral identification. Therefore, the identification and characterisation of novel phages remain a
24 challenge.

25 Results

26 We introduce Phables, a new computational method to resolve phage genomes from
27 fragmented viral metagenome assemblies. Phables identifies phage-like components in the
28 assembly graph, models each component as a flow network, and uses graph algorithms and
29 flow decomposition techniques to identify genomic paths. Experimental results of viral
30 metagenomic samples obtained from different environments show that Phables recovers on
31 average over 49% more high-quality phage genomes compared to existing viral identification
32 tools. Furthermore, Phables can resolve variant phage genomes with over 99% average
33 nucleotide identity, a distinction that existing tools are unable to make.

34 Availability and Implementation

35 Phables is available on GitHub at <https://github.com/Vini2/phables>.

36 Contact

37 vijini.mallawaarachchi@flinders.edu.au

38 Introduction

39 Bacteriophages (hereafter *phages*) are viruses that infect bacteria, which influence microbial
40 ecology and help modulate microbial communities (Edwards and Rohwer 2005; Rodriguez-
41 Valera et al. 2009). Phages are considered the most abundant biological entity on earth,
42 totalling an estimated 10^{31} particles (Comeau et al. 2008). Since their discovery by Frederick
43 Twort in 1915 (Twort 1915), phages have been isolated from many diverse environments (Keen
44 2015). When sequencing technologies were first developed, phage genomes were the first to be
45 sequenced due to their relatively small genome size (Sanger et al. 1977). With the advent of
46 second-generation sequencing technologies, the first metagenomic samples to be sequenced
47 were phages (Breitbart et al. 2002). The availability of advanced sequencing technologies has
48 facilitated the investigation of the effect of phages on the functions of microbial communities,
49 especially in the human body's niche areas. For example, phages residing in the human gut
50 have a strong influence on human health (Łusiak-Szelachowska et al. 2017) and impact
51 gastrointestinal diseases such as inflammatory bowel disease (IBD) (Norman et al. 2015). To
52 date, our understanding of the diversity of phages is limited, as most have not been cultured
53 due to the inherent difficulty of recovering phages from their natural environments. Although
54 countless millions of phage species are thought to exist, only 25,936 complete phage genomes
55 have been sequenced according to the INfrastructure for a PHAge REference Database
56 (INPHARED) (Cook et al. 2021) (as of the July 2023 update).

57 Metagenomics has enabled the application of modern sequencing techniques for the culture-
58 independent study of microbial communities (Hugenholtz, Goebel, and Pace 1998).

59 Metagenomic sequencing provides a multitude of sequencing reads from the genetic material in
60 environmental samples that are composed of a mixture of prokaryotic, eukaryotic, and viral
61 species. Metagenomic analysis pipelines start by assembling sequencing reads from
62 metagenomic samples into longer contiguous sequences that are used in downstream
63 analyses. Most metagenome assemblers (D. Li et al. 2015; Nurk et al. 2017; Namiki et al. 2012;
64 Peng et al. 2011) use de Bruijn graphs (P. A. Pevzner, Tang, and Waterman 2001) as the
65 primary data structure where they break sequencing reads into smaller pieces of length k
66 (known as ' k -mers') and represent k -mers as vertices and edges as overlaps of length $k-1$. After
67 performing several simplification steps, the final *assembly graph* represents sequences as
68 vertices and connection information between these sequences as edges (Nurk et al. 2017; V.
69 Mallawaarachchi, Wickramarachchi, and Lin 2020). Non-branching paths in the assembly graph

70 (paths where all vertices have an in-degree and out-degree of one, except for the first and last
71 vertices) are referred to as *unitigs* (Kececioglu and Myers 1995). Unitigs are entirely consistent
72 with the read data and belong to the final genome(s). Assemblers condense unitigs into
73 individual vertices and resolve longer optimised paths through the branches into contiguous
74 sequences known as *contigs* (Bankevich et al. 2012). As the contextual and contiguity
75 information of reads is lost in de Bruijn graphs, mutations in metagenomes with high strain
76 diversity appear as “*bubbles*” in the assembly graph where a vertex has multiple outgoing edges
77 (branches) which eventually converge as incoming edges into another vertex (P. A. Pevzner,
78 Tang, and Waterman 2001; Pavel A. Pevzner, Tang, and Tesler 2004). Assemblers consider
79 these bubbles as errors and consider one path of the bubble corresponding to the dominant
80 strain (Bankevich et al. 2012) or terminate contigs prematurely (D. Li et al. 2015). Moreover,
81 most metagenome assemblers are designed and optimised for bacterial genomes and fail to
82 recover viral populations with low coverage and genomic repeats (Roux et al. 2017; Sutton et al.
83 2019). However, previous studies have shown that contigs that are connected to each other are
84 more likely to belong to the same genome (V. Mallawaarachchi, Wickramarachchi, and Lin
85 2020; V. G. Mallawaarachchi, Wickramarachchi, and Lin 2020, 2021). Hence, the assembly
86 graph retains important connectivity and neighbourhood information within fragmented
87 assemblies. This concept has been successfully applied to develop tools such as GraphMB
88 (Lamurias et al. 2022), MetaCoAG (V. Mallawaarachchi and Lin 2022a, [b] 2022), and RepBin
89 (Xue et al. 2022), where the assembly graphs are utilised in conjunction with taxonomy-
90 independent metagenomic binning methods to recover high-quality metagenome-assembled
91 genomes (hereafter *MAGs*) of bacterial genomes. Moreover, assembly graphs have been used
92 for bacterial strain resolution in metagenomic data (Quince et al. 2021). However, limited
93 studies have been conducted to resolve phage genomes in metagenomic data, particularly viral
94 enriched metagenomes.

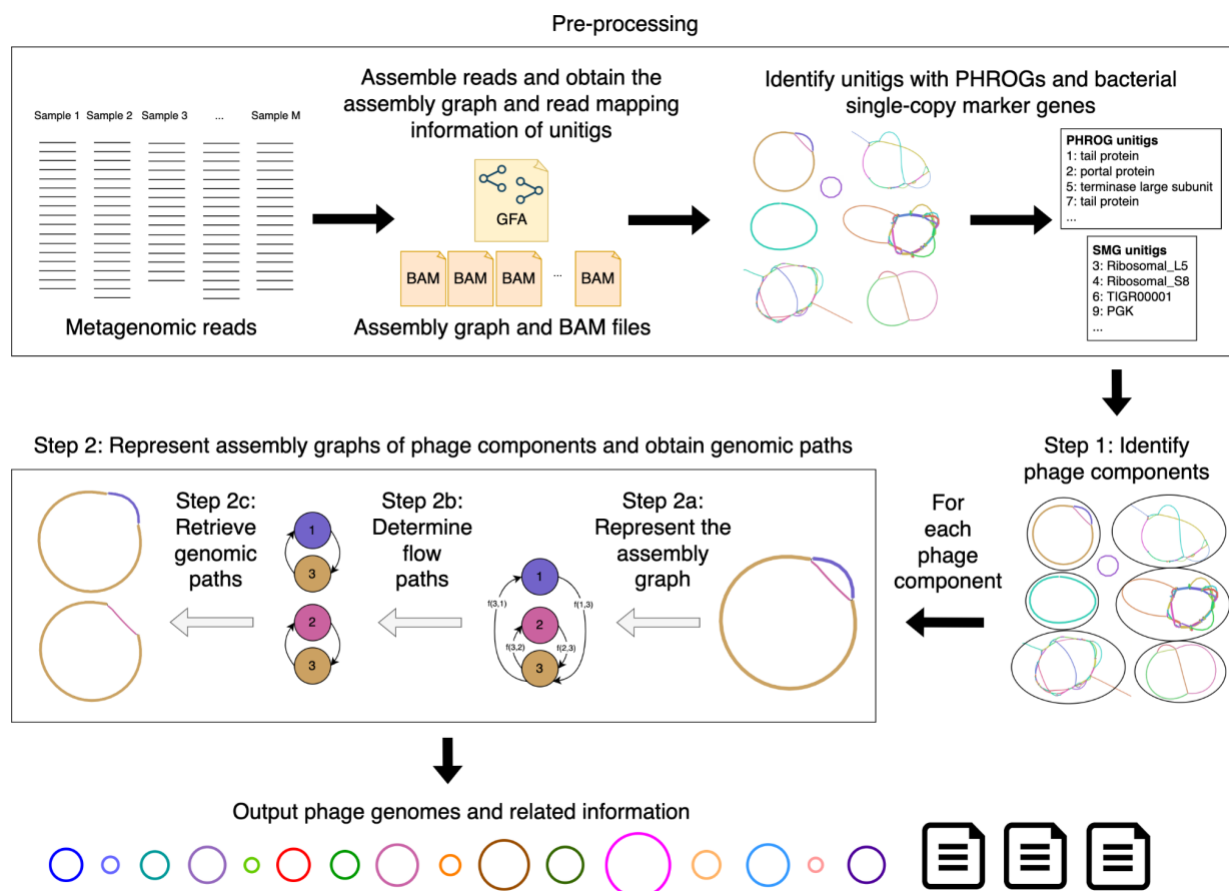
95 Computational tools have enabled large-scale studies to recover novel phages entirely from
96 metagenomic sequencing data (Simmonds et al. 2017) and gain insights into interactions with
97 their hosts (Nayfach, Páez-Espino, et al. 2021; M. J. Roach, McNair, et al. 2022; Hesse et al.
98 2022). While exciting progress has been made towards identifying new phages, viral dark
99 matter remains vast. Current methods are either too slow or result in inaccurate or incomplete
100 phage genomes. Generating high-quality phage genomes via *de novo* metagenome assembly is
101 challenging due to the modular and mosaic nature of phage genomes (Lima-Mendez,
102 Toussaint, and Leplae 2011; Hatfull 2008; Belcaid, Bergeron, and Poisson 2010). Repeat
103 regions can result in fragmented assemblies and chimeric contigs (Casjens and Gilcrease 2009;

104 Merrill et al. 2016). Hence, current state-of-the-art computational tools rely on the combination
105 of either more conservative tools based on sequence- and profile-based screening (e.g.
106 MetaPhinder (Jurtz et al. 2016)) or machine learning approaches based on nucleotide
107 signatures (e.g. Seeker (Auslander et al. 2020), refer to Table S1 in section 1 of the
108 Supplementary material). Resulting predictions are then evaluated using tools such as CheckV
109 (Nayfach, Camargo, et al. 2021) and VIBRANT (Kieft, Zhou, and Anantharaman 2020) to
110 categorise the predicted phages based on their completeness, contamination levels, and
111 possible lifestyle (virulent or temperate) (McNair, Bailey, and Edwards 2012). Due to the
112 supervised nature of the underlying approaches, most of these tools cannot characterise novel
113 viruses that are significantly different from known viruses. Moreover, the approach used by
114 these tools can be problematic with fragmented assemblies where contigs do not always
115 represent complete genomes. In an attempt to address this limitation, tools such as MARVEL
116 (Amgarten et al. 2018) and PHAMB (Johansen et al. 2022) were developed to identify viral
117 metagenome-assembled genomes (vMAGs) of phages from metagenomic data. These
118 programs rely on existing taxonomy-independent metagenomic binning tools such as MetaBAT2
119 (Kang et al. 2019) or VAMB (Nissen et al. 2021) and attempt to predict viral genome bins from
120 this output using machine learning techniques.

121 Metagenomic binning tools are designed to capture nucleotide and sequence coverage-specific
122 patterns of different taxonomic groups; therefore, sequences from viruses with low and uneven
123 sequence coverage are often inaccurately binned. Many metagenomic binning tools filter out
124 short sequences (e.g., shorter than 1,500 bp (Kang et al. 2019)), which further result in the loss
125 of essential regions in phage genomes that are often present as short fragments in the
126 assembly (Casjens and Gilcrease 2009). Moreover, most metagenomic binning tools struggle to
127 distinguish viruses from genetically diverse populations with high strain diversity and
128 quasispecies dynamics. These tools do not resolve the clustered sequences into contiguous
129 genomes and the bins produced often contain a mixture of multiple strains resulting in poor-
130 quality MAGs (Meyer et al. 2022). Existing solutions developed for viral quasispecies assembly
131 only consider one species at a time (Baaijens, Stougie, and Schönhuth 2020; Freire et al. 2021,
132 2022) and cannot be applied to complex metagenomes. Despite the recent progress, it is
133 challenging for currently available tools to recover complete high-quality phage genomes from
134 metagenomic data, and a novel approach is required to address this issue. The use of
135 connectivity information from assembly graphs could overcome these challenges (as shown in
136 previous studies on bacterial metagenomes (V. Mallawaarachchi and Lin 2022a, [b] 2022;
137 Lamurias et al. 2022)) to enable the recovery of high-quality phage genomes.

138 In this paper, we introduce Phables, a software tool that can resolve complete high-quality
139 phage genomes from viral metagenome assemblies. First, Phables identifies phage-like
140 components in the assembly graph using conserved genes. Second, using read mapping
141 information, graph algorithms and flow decomposition techniques, Phables identifies the most
142 probable combinations of varying phage genome segments within a component, leading to the
143 recovery of accurate phage genome assemblies (Figure 1). We evaluated the quality of the
144 resolved genomes using different assessment techniques and demonstrate that Phables
145 produces complete and high-quality phage genomes.

146 Materials and Methods



147

148 Figure 1: Phables workflow. Pre-processing: Assemble reads, obtain the assembly graph and
149 read mapping information, and identify unitigs with PHROGs and bacterial single copy marker
150 genes. Step 1: Identify phage components from the initial assembly. Step 2: For each phage

151 component, represent the assembly graph, determine the flow paths and retrieve the genomic
152 paths. Finally, output phage genomes and related information.

153 Here we present the overall workflow of Phables (Figure 1). Metagenomic reads from single or
154 multiple viral metagenomic samples are assembled, and the assembly graph and read mapping
155 information are obtained. The unitig sequences from the assembly graph are extracted and
156 screened for Prokaryotic Virus Remote Homologous Groups (PHROGs) (Terzian et al. 2021)
157 and bacterial single-copy marker genes. Phables identifies sub-graphs (known as *phage*
158 *components*) and resolves separate phage genomes from each phage component. Finally,
159 Phables outputs the resolved phage genomes and related information. Each step of Phables is
160 explained in detail in the following sections.

161 Pre-processing

162 The pre-processing step performed by Phables uses an assembly graph and generates the
163 read mapping information and the gene annotations required for Step 1 in the workflow. We
164 recommend Hecatomb (M. J. Roach, Beecroft, et al. 2022) to assemble the reads into contigs
165 and obtain the assembly graph. However, Phables will work with any assembly graph in
166 Graphical Fragment Assembly (GFA) format.

167 The unitig sequences are extracted from the assembly graph, and the raw sequencing reads
168 are mapped to the unitigs using Minimap2 (H. Li 2018) and Samtools (H. Li et al. 2009).
169 Phables uses CoverM (Woodcroft and Newell 2017) to calculate the read coverage of unitigs,
170 using the reads from all samples, and records the mean coverage (the average number of reads
171 that map to each base of the unitig).

172 Phables identifies unitigs containing Prokaryotic Virus Remote Homologous Groups (PHROGs)
173 (Terzian et al. 2021). PHROGs are viral protein families commonly used to annotate prokaryotic
174 viral sequences. MMSeqs2 (Steinegger and Söding 2017) is used to identify PHROGs in unitigs
175 using an identity cutoff of 30% and an e-value of less than 10^{-10} (by default).

176 Phables identifies unitigs containing bacterial single-copy marker genes. Most bacterial
177 genomes have conserved genes known as single-copy marker genes (SMGs) that appear only
178 once in a genome (Dupont et al. 2012; Albertsen et al. 2013). FragGeneScan (Rho, Tang, and
179 Ye 2010) and HMMER (Eddy 2011) are used to identify sequences containing SMGs. SMGs
180 are considered to be present if more than 50% (by default) of the gene length is aligned to the
181 unitig. The list of SMGs is provided in Table S2 in section 2 of the Supplementary material.

182 Step 1: Identify phage components

183 Phables identifies components from the final assembly graph where all of its unitigs do not have
184 any bacterial SMGs (identified from the preprocessing step) and at least one unitig contains one
185 or more genes belonging to a PHROG for at least one of the PHROG categories: *head and*
186 *packaging, connector, tail* and *lysis* which contain known phage structural proteins and are
187 highly conserved in tailed phages (Auslander et al. 2020) (refer to Figure S1 in section 3 of the
188 Supplementary material for an analysis of the PHROG hits to all known phage genomes). The
189 presence of selected PHROGs ensures the components are phage-like and represent potential
190 phage genomes. The absence of bacterial SMGs further ensures that the components are not
191 prophages. These identified components are referred to as *phage components*. Components
192 that are comprised of a single circular unitig (the two ends of the unitig overlap) or a single linear
193 unitig and that satisfy the above conditions for genes are considered *phage components* only if
194 the unitig is longer than the predefined threshold *minlength* that is set to 2,000 bp by default,
195 as this is the approximate lower bound of genome length for tailed phages (Luque et al. 2020).

196 Step 2: Represent assembly graphs of phage components and 197 obtain genomic paths

198 Step 2a: Represent the assembly graph

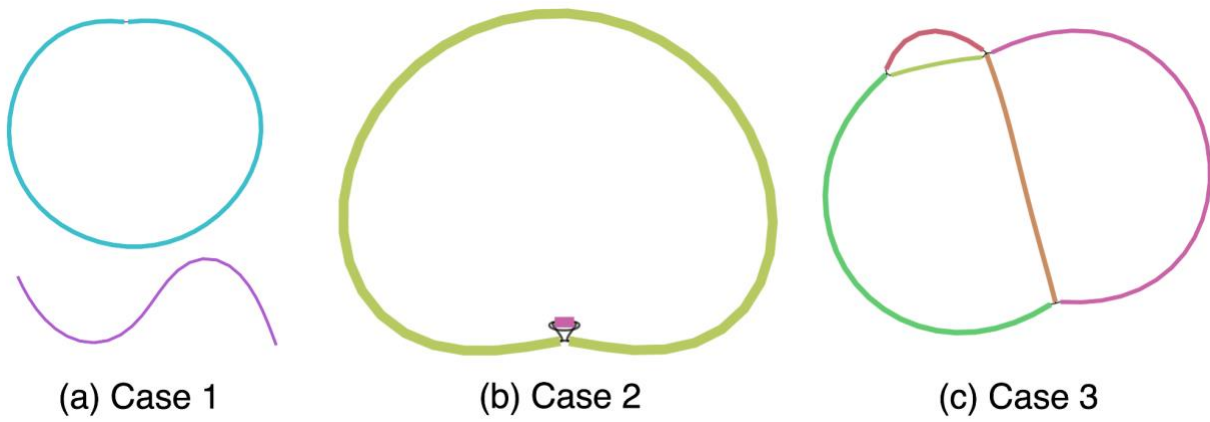
199 Following the definitions from STRONG (Quince et al. 2021), we define the assembly graph
200 $G = (V, E)$ for a phage component where $V = \{1, 2, 3, \dots, |V|\}$ is a collection of vertices
201 corresponding to unitig sequences that make up a phage component and directed edges
202 $E \in V \times V$ represent connections between unitigs. Each directed edge $(u^{d_1} \rightarrow v^{d_2})$ is defined
203 by a starting vertex u and an ending vertex v (the arrow denotes the direction of the overlap),
204 where $d_1, d_2 \in \{+, -\}$ indicates whether the overlap occurs between the original sequence,
205 indicated by a + sign or its reverse complement, indicated by a - sign.

206 The *weight* of each edge $(u^{d_1} \rightarrow v^{d_2})$ irrespective of the orientation of the edge, termed
207 $w_e(u \rightarrow v)$ is set to the minimum of the read coverage values of the two unitigs u and v . We
208 also define the *confidence* of each edge $(u^{d_1} \rightarrow v^{d_2})$ irrespective of whether the overlap occurs
209 between the original sequence or its reverse complement, termed $c_e(u \rightarrow v)$ is defined as the
210 number of paired-end reads spanning across $(u \rightarrow v)$. Here, the forward read maps to unitig u

211 and the reverse read maps to unitig v . We also define the confidence of paths $(t \rightarrow u \rightarrow v)$
212 termed $c_p(t \rightarrow u \rightarrow v)$ as the number of paired-end reads spanning across unitigs t and v .
213 Paired-end information has been used in previous studies for assembling viral quasispecies
214 (Freire et al. 2022; J. Chen, Zhao, and Sun 2018) to untangle assembly graphs. Moreover,
215 paired-end reads are widely used in manual curation steps to join contigs from metagenome
216 assemblies and extend them to longer sequences (L.-X. Chen et al. 2020). The more paired-
217 end reads map to the pair of unitigs, the more confident we are about the overlap represented
218 by the edge (refer to Figure S2 in section 4 of the Supplementary material for histograms of
219 edge confidence).

220 **Step 2b: Determine flow paths**

221 Phables models the graph of the phage component as a flow decomposition problem and obtain
222 the genomic paths with their coverage values calculated from the read coverages of unitigs and
223 read mapping information. We define three cases based on the number and arrangement of
224 unitigs present in the phage component as shown in Figure 2. Each case will be discussed in
225 detail in the following sub-sections.



226 (a) Case 1 (b) Case 2 (c) Case 3
227 Figure 2: Cases of phage components. (a) Case 1 represents a phage component with one
228 circular unitig or one linear unitig. (b) Case 2 represents a phage component with two circular
229 unitigs connected to each other. (c) Case 3 represents a phage component that is more
230 complex with multiple unitigs and multiple paths.

231 Case 1: Phage component consists of one circular unitig

232 When the phage component has only one linear/circular unitig longer than the predefined
233 threshold $minlength$, Phables considers this unitig as one genome. The genomic path is
234 defined as the unitig sequence itself.

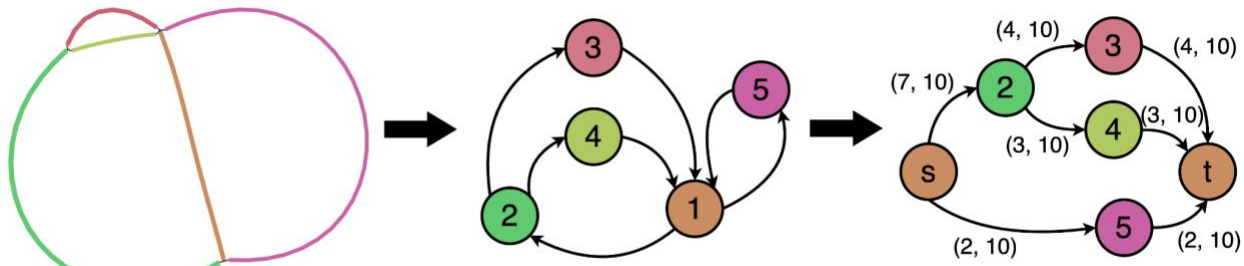
235 Case 2: Phage component consists of two circular unitigs

236 The phage components in case 2 have two circular unitigs connected together where at least
237 one is longer than the predefined threshold $minlength$. This is an interesting case as the
238 shorter unitig corresponds to the terminal repeats of phages. Some phages have double-
239 stranded repeats at their termini which are a few hundred base pairs in length and are exactly
240 the same in every virion chromosome (i.e. they are not permuted) (Casjens and Gilcrease
241 2009). The terminal repeats are generated by a duplication of the repeat region in concert with
242 packaging (Zhang and Studier 2004; Yeon-Bo Chung et al. 1990) (refer to Figure S3 in section
243 5 of the Supplementary material). This type of end structure could be overlooked when a phage
244 genome sequence is determined by shotgun methods because sequence assembly can merge
245 the two ends to give a circular sequence. Phables successfully resolves these terminal repeats
246 to form complete genomes.

247 To resolve the phage component in case 2, we consider the shorter unitig (shorter than
248 $minlength$) as the terminal repeat. Now we combine the original sequence of the terminal
249 repeat to the beginning of the longer unitig and the reverse complement of the terminal repeat to
250 the end of the longer unitig (refer to Figure S3 in section 5 of the Supplementary material). The
251 coverage of the path will be set to the coverage of the longer unitig.

252 Case 3: Phage component consists of three or more unitigs

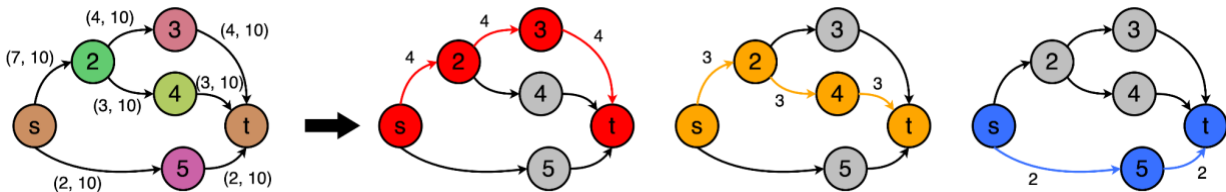
253 In case 3, we have more complex phage components where there are more than two unitigs
254 forming branching paths, and we model them as a minimum flow decomposition (MFD)
255 problem. The MFD problem decomposes a directed acyclic graph (DAG) into a minimum
256 number of source-to-sink ($s - t$) paths that explain the flow values of the edges of the graph
257 (Vatinlen et al. 2008; Dias et al. 2022). The most prominent applications of the MFD problem in
258 bioinformatics include reconstructing RNA transcripts (Shao and Kingsford 2017; Tomescu et al.
259 2013; Gatter and Stadler 2019) and viral quasispecies assembly (Baaijens, Stougie, and
260 Schönhuth 2020). The MFD problem can be solved using integer linear programming (ILP)
261 (Schrijver 1998).



262

263

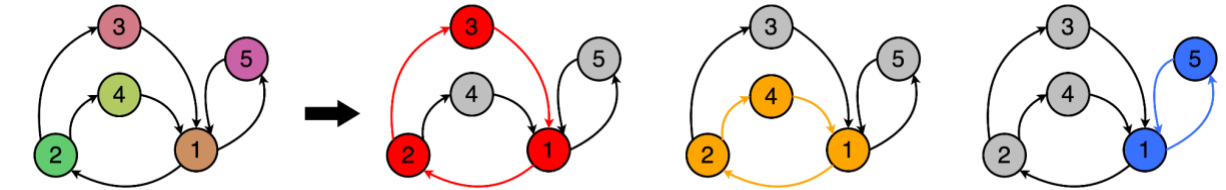
(a)



264

265

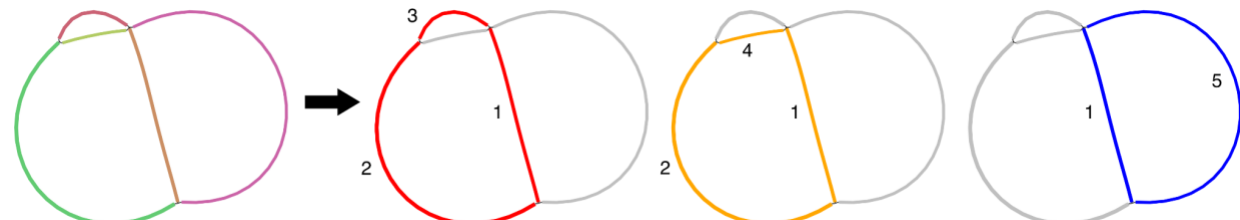
(b)



266

267

(c)



268

269

(d)

270

271

272

273

274

Figure 3: Example of a phage component (a) being modelled as a flow network and resolved into paths denoted using (b) flow network visualisation with flow values, (c) graph visualisation with directed edges and (d) Bandage (Wick et al. 2015) visualisation (with corresponding unitig numbers). Here three $s - t$ flow paths ($1 \rightarrow 2 \rightarrow 3$, $1 \rightarrow 2 \rightarrow 4$ and $1 \rightarrow 5$) can be obtained corresponding to three phage genomes. The arrows in (b) - (d) denote the resolution into 3 paths.

275 In the viral metagenomes, we have identified structures containing several phage variant
276 genomes, that are similar to viral quasispecies often seen in RNA viruses (Domingo and
277 Perales 2019). Hence, Phables models each of the remaining phage components as an MFD
278 problem and uses the MFD-ILP implementation from Dias *et al.* (Dias *et al.* 2022). MFD-ILP
279 finds a $FD(\mathcal{P}, w)$ with a set of $s - t$ flow paths \mathcal{P} and associated weights w such that the
280 number of flow paths is minimized. These flow paths represent possible genomic paths. An
281 example of a phage component with possible paths is shown in Figure 3.

282 First, we convert the assembly graph of the phage component into a DAG. We start by
283 removing *dead-ends* from G . We consider a vertex to be a *dead-end* if it has either no incoming
284 edges or no outgoing edges, which arise due to errors at the start or end of reads that can
285 create protruding chains of deviated edges (Bankevich *et al.* 2012). Dead-ends are particularly
286 problematic in later steps of Phables as they can affect the continuity of genomic paths. Hence,
287 their removal ensures that all the possible paths in the graph form closed cycles. We eliminate
288 dead-ends by recursively removing vertices with either no incoming edges or no outgoing
289 edges. Note that removing one dead-end can cause another vertex that is linked only to the
290 removed one to become a dead-end, hence the removal process is done recursively.

291 Since a case 3 phage component forms a cyclic graph as shown in Figure 3 (a), we have to
292 identify a vertex to represent the source/sink (referred to as *st*) in order to convert the graph to a
293 DAG and model it as a flow network. Starting from every vertex (*source*), we conduct a breadth-
294 first-search and identify an iterator, $(level, vertices)$, where *vertices* is the non-empty list of
295 vertices at the same distance *level* from the *source*. The method that generates this iterator is
296 known as *bfs_layers* and we use the NetworkX implementation
297 (https://networkx.org/documentation/stable/reference/algorithms/generated/networkx.algorithms.traversal.breadth_first_search.bfs_layers.html#networkx.algorithms.traversal.breadth_first_search.bfs_layers). We extract the vertices in the final layer and check if their successors are equal
300 to *source*. If this condition holds for some vertex in G , we consider this vertex to be the *st* vertex
301 of G . If more than one vertex satisfies the condition to be a *st* vertex, then we pick the vertex
302 corresponding to the longest unitig as the *st* vertex. This process is carried out to find a vertex
303 common to the flow paths (refer to Algorithm S1 in section 6 of the Supplementary material). As
304 an example, consider vertex 1 in Figure 3 (a). When we do a breadth-first-search starting from
305 vertex 1, the vertices in the last layer in our iterator will be 3 and 4. The successor of both 3 and
306 4 is vertex 1. Since the successors of the vertices in the last layer are the same as the starting
307 vertex, we consider vertex 1 as the *st* vertex.

308 The edges of G that are weighted according to unitig coverage, may not always satisfy the
309 conservation of flow property because of uneven sequencing depths at different regions of the
310 genomes (Peng et al. 2012; Gunasekera et al. 2021). Hence, we use inexact flow networks
311 which allow the edge weights to belong to an interval. Once we have identified a st vertex, we
312 separate that vertex into two separate vertices for the source s and sink t . We create an inexact
313 flow network $G_f = (V, E, f, \bar{f})$ from s to t and model the rest of the vertices and edges in G . For
314 example, in Figure 3 (b) vertex 1 is broken into two vertices s and t , and the network flows from s
315 to t . For every edge $(u, v) \in E$ we have associated two positive integer values $f_{uv} \in f$ and
316 $\bar{f}_{uv} \in \bar{f}$, satisfying $f_{uv} \leq \bar{f}_{uv}$ where $f_{uv} = w_e(u \rightarrow v)$, $\bar{f}_{uv} = \lfloor \alpha \times cov_{max} \rfloor$, $\alpha \geq 1$ is the
317 coverage multiplier parameter (1.2 by default) and cov_{max} is the maximum coverage of a unitig
318 in the phage component. In Figure 3 (b), each edge has two values (f_{uv}, \bar{f}_{uv}) that define the
319 flow interval for the inexact flow network G_f . This modelling ensures that the flow through each
320 edge is bounded by a relaxed interval between the edge weight and the maximum coverage
321 within the component. For example, in Figure 3 (b), the edge $(2 \rightarrow 3)$ has a weight of 4 (which is
322 the minimum of the read coverage values of the two unitigs 2 and 3 obtained from Step 2a).
323 $\alpha = 1.2$ and $cov_{max} = 9$ for the component. Hence, we set $f_{uv} = 4$ and $\bar{f}_{u,v} = 10$.

324 Next, we define a set of simple paths $\mathcal{R} = \{R_1, R_2, R_3, \dots, R_l\}$ where the edges that form each
325 path have paired-end reads spanning across them, i.e. $c_e(u \rightarrow v) \geq mincov$. Enforcing these
326 paths to contain paired-end reads ensures that genuine connections are identified and reflected
327 in at least one decomposed path. For example, in Figure 3 (b), the edge $(2 \rightarrow 3)$ has 4 paired-
328 end reads spanning across the edge. Hence, we add the path $R_1 = (2, 3)$ to \mathcal{R} . Moreover, for a
329 path $t \rightarrow u \rightarrow v$ passing through the junction u (where the in-degree and out-degree are non-
330 zero), we add the path $R_j = (t, u, v)$ to \mathcal{R} , if $c_p(t \rightarrow u \rightarrow v) \geq mincov$ or if
331 $|w_e(t \rightarrow u) - w_e(u \rightarrow v)|$ is less than a predefined threshold $cov_{tolerance}$ (100 by default). This
332 allows Phables to specify longer subpaths across complex junctions.

333 Now we model our inexact flow network G_f as a minimum inexact flow decomposition (MIFD)
334 problem and determine a minimum-sized set of $s - t$ paths $\mathcal{P} = (P_1, P_2, P_3, \dots, P_k)$ and
335 associated weights $w = (w_1, w_2, w_3, \dots, w_k)$ with each $w_i \in \mathbb{Z}^+$ where the following conditions
336 hold.

337

$$f_{uv} \leq \sum_{i \in \{1, \dots, k\} \text{ s.t. } (u, v) \in P_i} w_i \leq \bar{f}_{uv} \quad \forall (u, v) \in E$$

1. $\forall R_j \in \mathcal{R}, \exists P_i \in \mathcal{P}$ such that R_j is a subpath of P_i

338 1. $f_{uv} \leq \sum_{i \in \{1, \dots, k\} \text{ s.t. } (u, v) \in P_i} w_i \leq \bar{f}_{uv} \quad \forall (u, v) \in E$
339 2. $\forall R_j \in \mathcal{R}, \exists P_i \in \mathcal{P}$ such that R_j is a subpath of P_i

340 A path P_i will consist of unitigs with orientation information. The weight w_i will be the coverage of
341 the genome represented by the path P_i .

342 Step 2c: Retrieve genomic paths

343 The flow paths obtained from cases 1 and 2 described in the previous section are directly
344 translated to genomic paths based on the unitig sequences. In case 3, we get $s - t$ paths from
345 the flow decomposition step (as shown in Figure 3). The paths longer than the predefined
346 threshold $minlength$ and have a predefined coverage threshold of $mincov$ (10 by default) or
347 above are retained. For each remaining path, we remove t from the path as s and t are the same
348 vertex and combine the nucleotide sequences of the unitigs corresponding to the vertices and
349 the orientation of edges in the flow path (refer to Figure 3 (c) and (d)). Once the genomic paths
350 of phage components are obtained, we record the constituent unitigs, path length (in bp),
351 coverage (i.e., the flow value of the path) and the GC content of each genomic path.

352

353 Experimental Design

354 Simulated phage dataset

355 We simulated reads from the following four phages with the respective read coverage values
356 and created a simulated phage dataset (referred to as **simPhage**) to evaluate Phables.

357 1. Enterobacteria phage P22 (AB426868) - 100×
358 2. Enterobacteria phage T7 (NC_001604) - 150×
359 3. Staphylococcus phage SAP13 TA-2022 (ON911718) - 200×
360 4. Staphylococcus phage SAP2 TA-2022 (ON911715) - 400×

361 The Staphylococcus phage genomes have an average nucleotide identity (ANI) of 96.89%.
362 Paired-end reads were simulated using InSilicoSeq (Gourlé et al. 2019) with the predefined
363 MiSeq error model. We used metaSPAdes (Nurk et al. 2017) from SPAdes version 3.15.5 to
364 assemble the reads into contigs and obtain the assembly graph for the simPhage dataset.
365 Tables S3 and S5 in section 7 of the Supplementary material summarise the details of the
366 simulations and assemblies.

367 Real datasets

368 We tested Phables on the following real viral metagenomic datasets available from the National
369 Center for Biotechnology Information (NCBI).

370 1. Water samples from Nansi Lake and Dongping Lake in Shandong Province, China
371 (NCBI BioProject number PRJNA756429), referred to as **Lake Water**
372 2. Soil samples from flooded paddy fields from Hunan Province, China (NCBI BioProject
373 number PRJNA866269), referred to as **Paddy Soil**
374 3. Wastewater virome (NCBI BioProject number PRJNA434744), referred to as
375 **Wastewater**
376 4. Stool samples from patients with IBD and their healthy household controls (NCBI
377 BioProject number PRJEB7772) (Norman et al. 2015), referred to as **IBD**
378 All the real datasets were processed using Hecatomb version 1.0.1 to obtain a single assembly
379 graph for each dataset (M. J. Roach, Beecroft, et al. 2022). Tables S3 - S5 in section 7 of the
380 Supplementary material summarise the information about the datasets and their assemblies.

381 **Tools benchmarked**

382 We benchmarked Phables with PHAMB (Johansen et al. 2022), a viral identification tool that
383 predicts whether MAGs represent phages and outputs genome sequences. PHAMB takes
384 binning results from a metagenomic binning tool and predicts bins that contain bacteriophage
385 sequences. The MAGs for PHAMB were obtained by running VAMB (version 3.0.8), a binning
386 tool that does not rely on bacterial marker genes, in co-assembly mode on the original contigs
387 with the author-recommended parameter `--minfasta 2000` and the `--cuda` flag. The
388 commands used to run all the tools can be found in section 8 of the Supplementary material.

389 **Evaluation criteria**

390 **Evaluation criteria for binning tools**

391 The resolved genomes from Phables and identified MAGs from PHAMB were evaluated using
392 CheckV version 1.0.1 (Nayfach, Camargo, et al. 2021) (with reference database version 1.5)
393 which compares bins against a large database of complete viral genomes. We compare the
394 following metrics from the CheckV results.

- 395 1. CheckV viral quality
- 396 2. Completeness of sequences - number of sequences with >90% completeness
- 397 3. Contamination of sequences - number of sequences with <10% contamination
- 398 4. The number and length distribution of sequences with the following warnings
 - 399 a. Contig >1.5x longer than expected genome length
 - 400 b. High kmer_freq may indicate a large duplication

401 Since PHAMB predicts all viral bins, we only consider the bins from PHAMB that contain the
402 contigs corresponding to the unitigs recovered by Phables for a fair comparison.

403 **Evaluation criteria for resolved genomes**

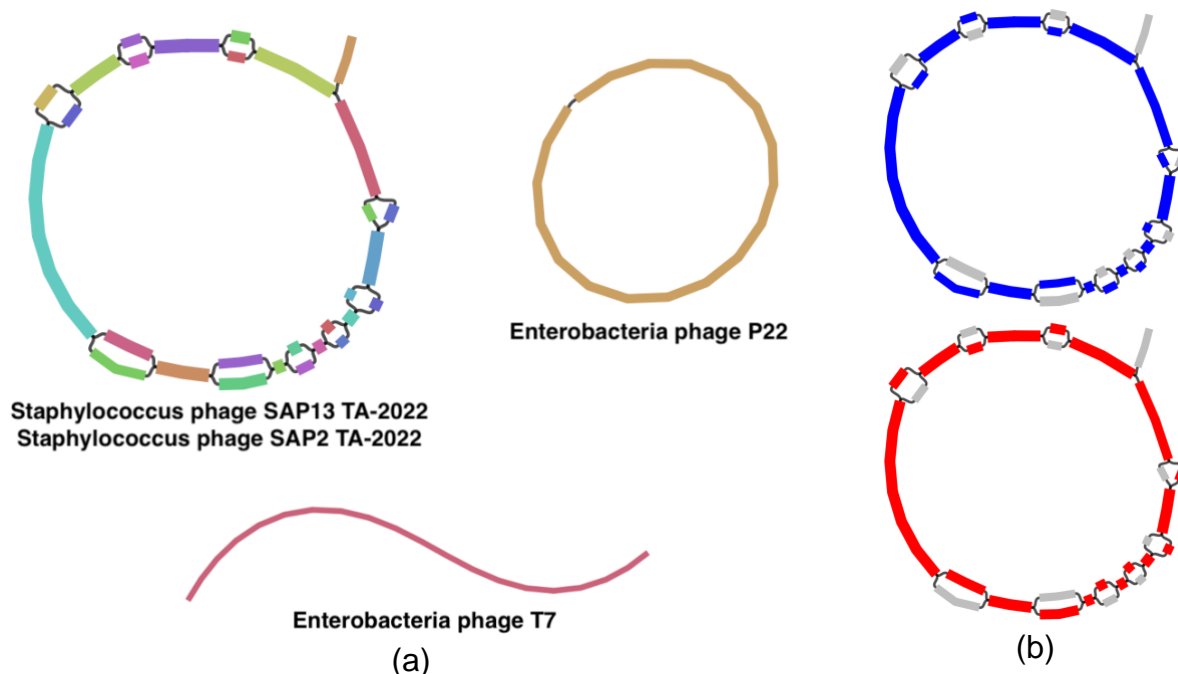
404 The number of components resolved by Phables for each case was recorded. The viral quality
405 of the resolved genomes and the unitigs and contigs contained in the corresponding genomic
406 paths were evaluated using CheckV version 1.0.1 (Nayfach, Camargo, et al. 2021). Since the
407 reference genomes for the simPhage dataset were available, we evaluated the resolved
408 genomes using metaQUAST (Mikheenko, Saveliev, and Gurevich 2016).

409 Results

410 Benchmarking results on the simulated phage dataset

411 We first benchmarked Phables using the simPhage dataset. We evaluated the resolved phage
412 genomes using metaQUAST (Mikheenko, Saveliev, and Gurevich 2016). We analysed the
413 genome coverage from metaQUAST and the coverage values reported by Phables. Figure 4
414 denotes the assembly graph (Bandage visualisation) of the simPhage dataset and how Phables
415 resolved the complex case 3 component containing Staphylococcus phages.

416



417

418 Figure 4: Visualisation of the (a) assembly graph from the simPhage with phage components
419 and (b) resolution of two paths (red and blue) from the Staphylococcus phage component.

420

421 Phables recovered the two Staphylococcus phage genomes with over 92% genome
422 completeness (refer to Table 1). The slightly low genome coverage for Staphylococcus phage
423 SAP2 TA-2022 may have been due to the omission of the dead-end which was not properly

424 assembled. Moreover, Phables has recovered the circular genome of Enterobacteria phage P22
425 and the linear genome of Enterobacteria phage T7 as well. According to Table 1, the coverage
426 values reported from Phables are similar or close to the actual simulated coverage values of the
427 genomes. VAMB failed to run on this dataset as there were fewer contigs than the minimum
428 possible batch size and hence PHAMB could not be run.

429

430 Table 1: Evaluation results for the genomes resolved from Phables for the simPhage dataset

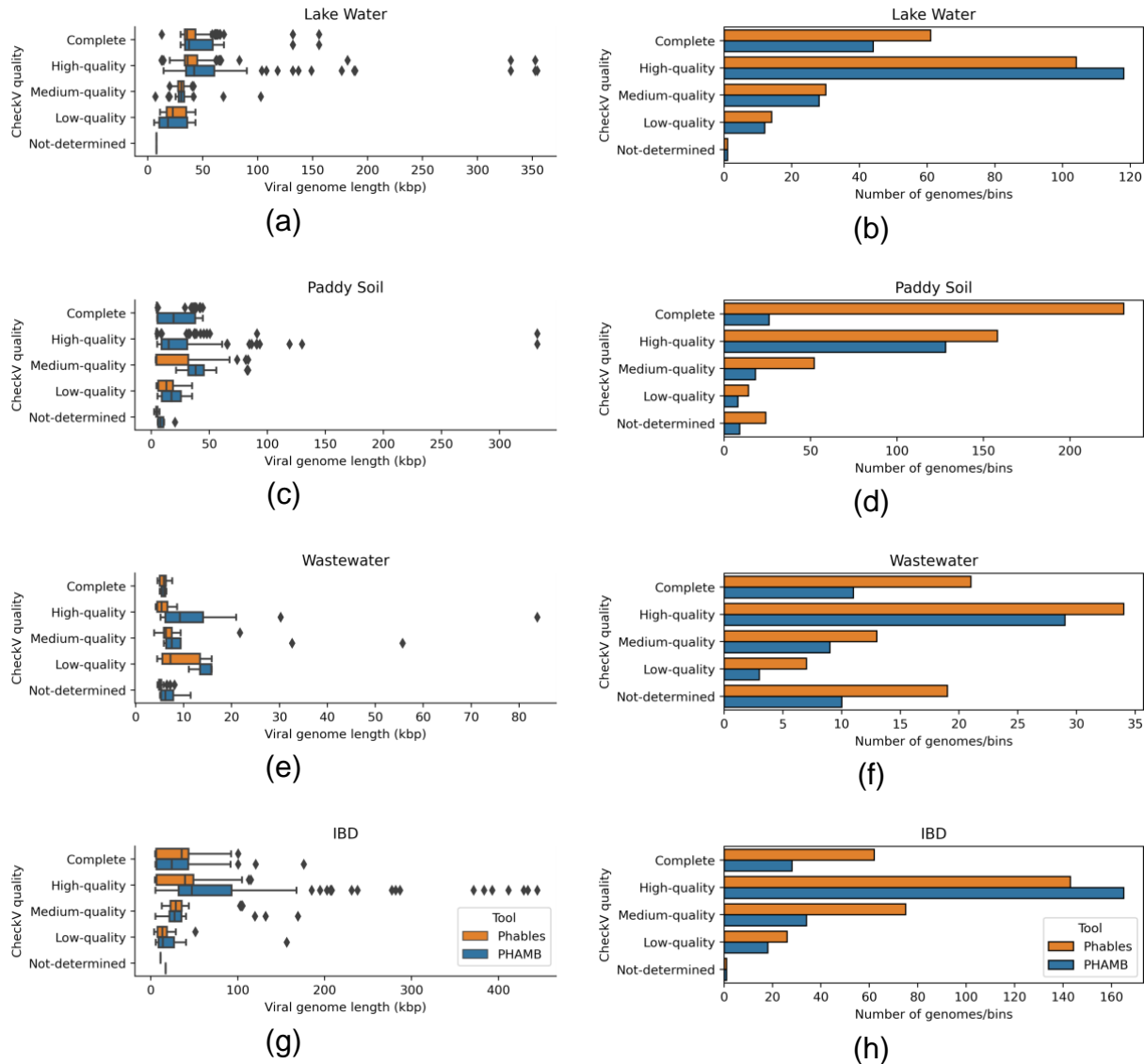
| Genome | Simulated coverage | Phables predicted coverage | Genome coverage (%) |
|------------------------------------|--------------------|----------------------------|---------------------|
| Enterobacteria phage P22 | 100 | 100 | 99.947 |
| Enterobacteria phage T7 | 150 | 150 | 99.599 |
| Staphylococcus phage SAP13 TA-2022 | 200 | 206 | 100 |
| Staphylococcus phage SAP2 TA-2022 | 400 | 401 | 92.406 |

431

432 Benchmarking results on the real datasets

433 Phables resolves unitigs within phage components to produce multiple complete and high-
434 quality genomes from the viral metagenomes (Figure 5). The genome quality of Phables results
435 was compared with the viral-MAG prediction tool PHAMB (Johansen et al. 2022) and evaluated
436 using CheckV (Nayfach, Camargo, et al. 2021). Figure 5 denotes the comparison of genome
437 length distributions and genome/bin counts of different CheckV quality categories for Phables
438 and PHAMB results. Unlike Phables, PHAMB has produced genomes with longer sequences as
439 shown in Figures 5 (a), (c), (e) and (g), because PHAMB combines all the contigs in a bin to
440 form one long sequence. As denoted in Figures 5 (b), (d), (f) and (h), Phables has recovered
441 the greatest number of complete and high-quality genomes combined for all the datasets; 165 in
442 Lake Water, 389 in Paddy Soil, 55 in Wastewater and 205 in IBD, with 49.54% more genomes
443 recovered than PHAMB on average.

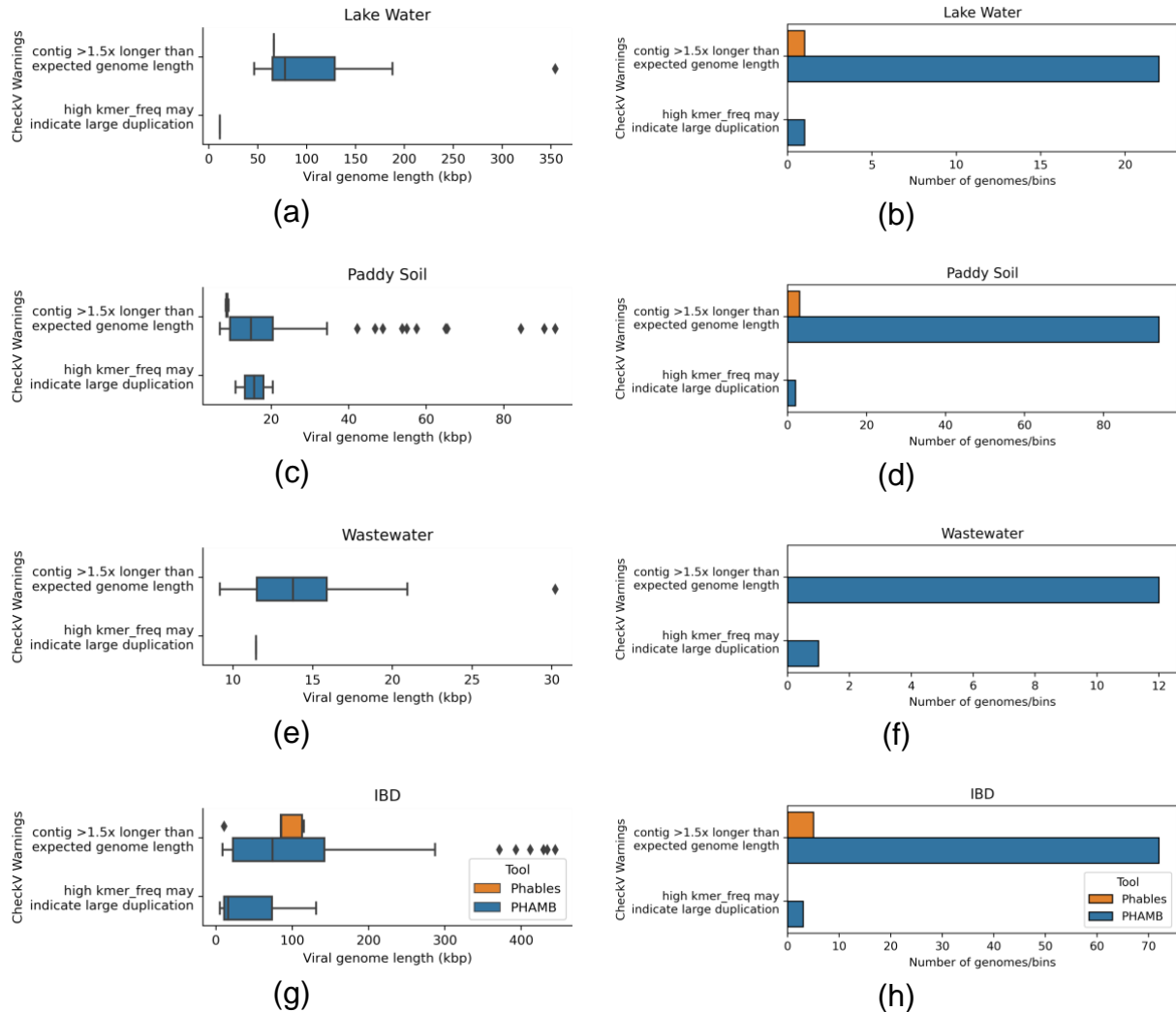
444



445

446 Figure 5: Genome length distribution (first column of figures) and abundance of genomes
 447 (second column of figures) belonging to different CheckV quality categories identified by
 448 Phables (denoted in orange) and PHAMB (Johansen et al. 2022) (denoted in blue) for the viral
 449 metagenomic datasets Lake Water, Paddy soil, Wastewater, and IBD.

450



451

452 Figure 6: Genome length distribution (first column of figures) and abundance of genomes
 453 (second column of figures) having the selected CheckV warnings from Phables (denoted in
 454 orange) and PHAMB (Johansen et al. 2022) (denoted in blue) results for the viral metagenomic
 455 datasets Lake Water, Paddy soil, Wastewater, and IBD.

456 Phables accurately recovers short sequences such as terminal repeats that are challenging for
 457 metagenomic binning tools to recover using the assembly graph and produces high-quality
 458 genomes. We observed that VAMB incorrectly binned the majority of the short sequences,
 459 which reduced the quality of PHAMB results. For example, the repeat sequences in the case 2
 460 phage components identified by Phables had a mean length of 600 bp in Lake Water, 649 bp in
 461 Paddy Soil, 511 bp in Wastewater and 638 bp in IBD datasets (refer to Table S6 in section 9 of
 462 the Supplementary material for exact lengths of the sequences). All of these short sequences,

463 except for those from the IBD dataset were found in a different bin than the bin of their
464 connected longer sequence in the PHAMB results (8 out of 8 in Lake Water, 2 out of 2 in Paddy
465 Soil and 1 out of 1 in Wastewater). Phables recovered these short repeat sequences along with
466 their connected longer sequences within a phage component using the connectivity information
467 of the assembly graph.

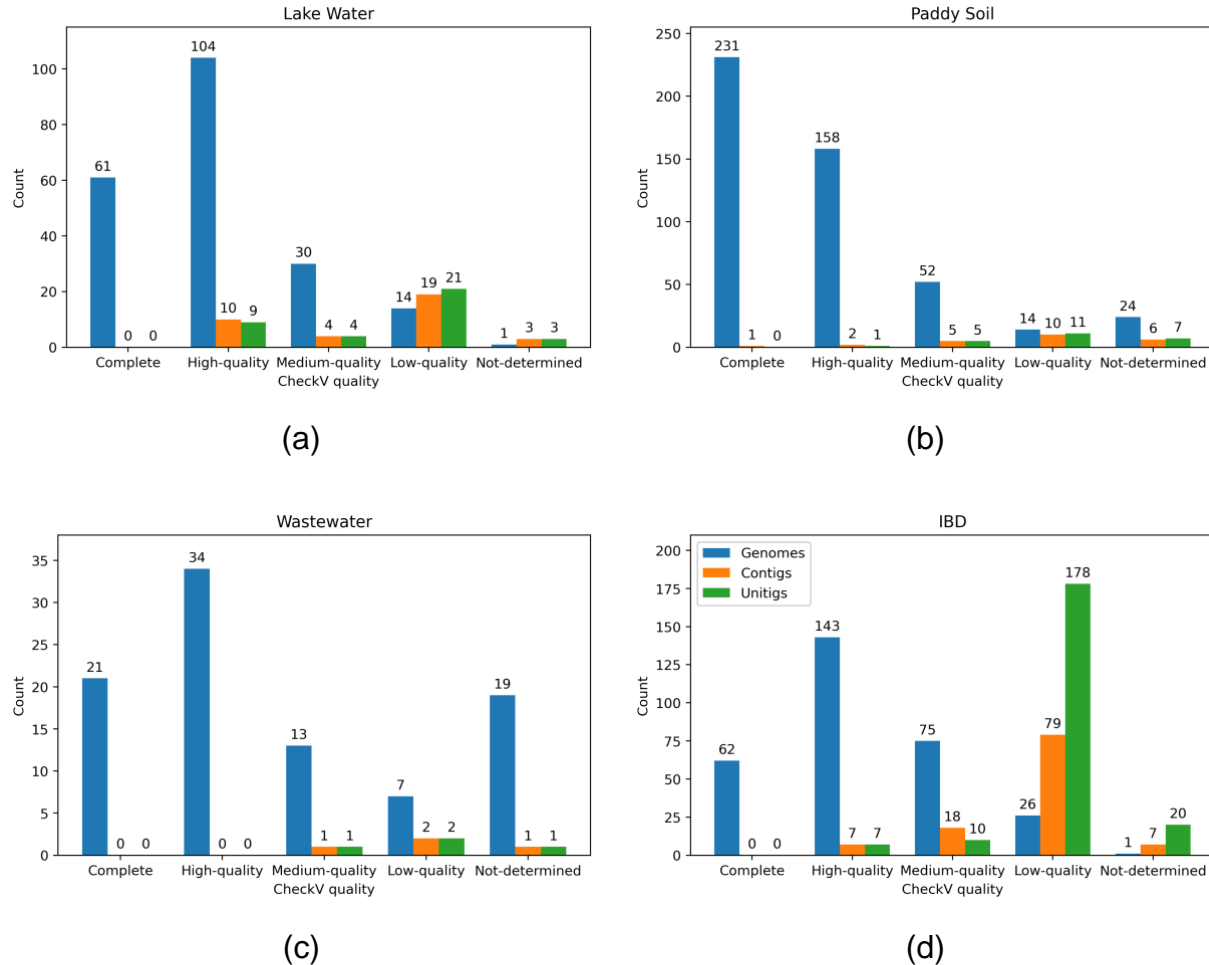
468 Phables resulted in a high number of low-quality genomes as determined by CheckV in the
469 Wastewater dataset compared to the other datasets (Figure 5 (f)). A possible reason for this is
470 that these may be novel phages (as they contain conserved phage markers even though
471 CheckV categorises them as “low-quality” or “not-determined”), and so they are not yet present
472 in the databases that CheckV relies on.

473 PHAMB does not carry out any resolution steps when combining the contigs of identified MAGs,
474 which results in erroneous genome structures, high levels of contamination and duplications
475 within genomes because of the presence of multiple variant genomes. Such duplications are
476 identified from the warnings reported by CheckV. Hence, we evaluated the number and length
477 distribution of sequences having CheckV warnings and the results are shown in Figure 6.
478 PHAMB has produced the highest number of genomes with CheckV warnings and produced
479 some very long genomes (~355 - 485 kbp as shown in Figures 6 (a) and (g)), suggesting the
480 combination of two or more variant genomes together in a bin. Only a few genomes produced
481 from Phables (5 or less) contain CheckV warnings (refer to Table S8 in section 10 of the
482 Supplementary material for the exact number of genomes with warnings). These results show
483 that Phables accurately recovers variant genomes including regions like terminal repeats from
484 viral metagenomic samples and produces more high-quality/complete genomes compared to
485 existing state-of-the-art tools.

486 Components resolved and comparison of resolved genomes

487 The number of phage components resolved by Phables under each case was recorded for all
488 the datasets (refer to Table S7 in section 9 of the Supplementary material for the exact counts).
489 Most of the resolved components belong to either case 1 with a single circular unitig or case 2
490 with the terminal repeat. When resolving case 2 components, Phables provides information
491 regarding terminal repeats such as the length of the repeat region, that will be overlooked by
492 other tools. Except for the IBD dataset, Phables was able to resolve all the case 3 phage
493 components from the rest of the datasets. In a few cases, the case 3 phage components could

494 not be resolved because Phables was unable to find a *st* vertex for these very complex bubbles
495 (refer to Figure S8 in section 11 of the Supplementary material for examples of unresolved
496 phage components).



497

498 Figure 7: Counts of resolved genomes of Phables, unitigs and contigs included in case 2 and 3
499 phage components with different CheckV qualities in the viral metagenomic datasets Lake
500 Water, Paddy soil, Wastewater, and IBD.

501

502 Assemblers attempt to resolve longer paths in the assembly graph by connecting unitigs to form
503 contigs (Bankevich et al. 2012; Kolmogorov et al. 2019). However, they are still unable to
504 resolve complete genomes for complex datasets due to the mosaic nature of phage genomes
505 and produce fragmented assemblies. Phables can be used to resolve these problematic contigs

506 (or unitigs) and obtain high-quality genomes. Figure 7 denotes the comparison of CheckV
507 quality of the genomes resolved in Phables and the unitigs and contigs included in the cases 2
508 and 3 phage components. The most complete and high-quality sequences can be found as
509 genomes (61 and 104 for Lake Water, 231 and 158 for Paddy Soil, 21 and 34 for Wastewater,
510 and 62 and 143 for IBD, respectively). In contrast, most medium- and low-quality genomes can
511 be found from contigs and unitigs. Hence, genomes resolved using Phables have higher quality
512 and will be better candidates for downstream analysis than contigs.

513 We compared the similarity between the genomes recovered within each case 3 phage
514 components for the IBD dataset using *pyani* (Pritchard et al. 2015), pyGenomeViz (Shimoyama
515 2022) and MUMmer (Marçais et al. 2018) (refer to section 12 of the Supplementary material for
516 the detailed results). The average nucleotide identity (ANI) analysis revealed that the genomes
517 resolved had over 95% ANI with some genomes having over 99% ANI and over 85% alignment
518 coverage. Moreover, as shown in Figure S10 in the Supplementary material, the mosaic
519 genome structure can be clearly seen where some unitigs are shared between genomes and
520 some genomes have unique unitigs. Depending on the size and location within a specific
521 genome, these unitigs potentially correspond to functional modules. Hence, Phables can
522 resolve highly similar variant genomes with mosaic genome structures that the assemblers are
523 unable to distinguish.

524 Phage components from other assembly methods

525 We extended our testing of Phables with co-assemblies obtained from other metagenome
526 assemblers including metaSPAdes (Nurk et al. 2017) and MEGAHIT (D. Li et al. 2015) to show
527 that the components with bubbles observed in the assembly graph are not an artefact of the
528 assembly approach used in Hecatomb. Co-assembly is conducted by combining reads from
529 multiple metagenomes and assembling them together, which increases the sequencing depth
530 and provides sufficient coverage for low-abundance genomes to be recovered (Delgado and
531 Andersson 2022). However, this becomes a computationally intensive approach as the number
532 of samples increases, and hence we have limited the results to just the Lake Water dataset. The
533 results are provided in section 13 of the Supplementary material and show that the phage
534 component structures are still present in the assemblies and were correctly resolved by
535 Phables, producing more high-quality genomes than PHAMB.

536 Implementation and resource usage

537 The source code of Phables was implemented using Python 3.10.12 and is available as a
538 pipeline (including all the preprocessing steps) developed using Snakemake (M. Roach et al.
539 2022). The commands used to run all the software can be found in section 8 of the
540 Supplementary material. The running times of Phables core methods and including the
541 preprocessing steps were recorded for all the datasets and can be found in Tables S10 and S11
542 in section 14 of the Supplementary material. The core methods of Phables can be run in under
543 2 minutes with less than 4 gigabytes of memory for all the datasets.

544 Phables uses a modified version of the MFD-ILP implementation from Dias et al. (Dias et al.
545 2022) which supports inexact flow decomposition with subpath constraints. Gurobi version
546 10.0.2 was used as the ILP solver. To reduce the complexity of the ILP solver, the maximum
547 number of unitigs in a phage component to be solved was limited to 200.

548 Discussion

549 The majority of the existing viral identification tools rely on sequence similarity- and profile-
550 based approaches, only identifying whether assembled sequences are of viral origin, and
551 cannot produce complete and high-quality phage genomes. Viral binning tools have been able
552 to overcome these shortcomings up to a certain extent by producing viral MAGs, but these
553 MAGs are fragmented and do not represent continuous genomes. Generally, the assembly
554 process produces many short contigs where some represent regions which while important are
555 challenging to resolve in phages, such as terminal repeat regions. These short contigs are
556 discarded or binned incorrectly by viral binning tools, producing incomplete MAGs. Moreover,
557 the mosaic genome structures of phage populations are a widely-documented phenomenon
558 (Lima-Mendez, Toussaint, and Leplae 2011; Hatfull 2008; Belcaid, Bergeron, and Poisson
559 2010), and cannot be resolved by existing assemblers and binning tools. The resulting MAGs
560 may contain multiple variant genomes assembled together and hence have high contamination.

561 Here, we introduce Phables, a new tool to resolve complete and high-quality phage genomes
562 from viral metagenome assemblies using assembly graphs and flow decomposition techniques.
563 We studied the assembly graphs constructed from different assembly approaches and different
564 assembly software and consistently observed phage-like components with variation (*phage*
565 *components*). Phables models the assembly graphs of these components as a minimum flow

566 decomposition problem using read coverage and paired-end mapping information and recovers
567 the genomic paths of different variant genomes. Experimental results confirmed that Phables
568 recovers complete and high-quality phage genomes with mosaic genome structures, including
569 important regions such as terminal repeats. However, Phables can identify certain plasmids as
570 phages (e.g. *phage-plasmids* (Ravin, Svarchevsky, and Dehò 1999; Pfeifer et al. 2021; Pfeifer,
571 Bonnin, and Rocha 2022)) because they can encode proteins homologous to phage sequences
572 (refer to section 15 in the Supplementary material). Hence, if users run mixed-microbial
573 communities through Phables, further downstream analysis is required to ensure that the
574 predicted genomes do not include plasmids.

575 Decomposing assembly graphs has become a popular method to untangle genomes and
576 recover variant genomes from assemblies and while we have successfully used it to obtain
577 mostly circular phage genomes, further work needs to be conducted to handle viral
578 metagenomes and recover the range of phage genomes. In the future, we intend to add support
579 for long-read assemblies from dedicated metagenome assemblers that will enable Phables to
580 enforce longer subpaths that will span across more sequences during the flow decomposition
581 modelling. We also intend to extend the capabilities of Phables to recover linear phage
582 genomes and explore the avenues for recovering high-quality eukaryotic viral genomes from
583 metagenomes.

584 Data and Code Availability

585 All the real datasets containing raw sequencing data used for this work are publicly available
586 from their respective studies. The Lake Water dataset was downloaded from NCBI with
587 BioProject number PRJNA756429, the Paddy Soil dataset from BioProject number
588 PRJNA756429, the Wastewater dataset from BioProject number PRJNA434744, and the whole
589 genome sequencing runs of the IBD data from BioProject number PRJEB7772. The sequencing
590 reads for the simPhage dataset, all the assembled data and results from all the tools are
591 available on Zenodo at <https://zenodo.org/record/8137197>.

592 The code of Phables is freely available on GitHub under the MIT license and can be found at
593 <https://github.com/Vini2/Phables>. All analyses in this study were performed using Phables
594 v.1.1.0 with default parameters. Phables is also available as a package on bioconda at
595 <https://anaconda.org/bioconda/phables> and on PyPI at <https://pypi.org/project/phables/>.

596 Author Contributions

597 V.M. designed the methods, developed the software, performed all analyses and wrote the
598 paper. M.J.R. preprocessed the datasets. M.J.R. and P.D. assisted with developing the pipeline,
599 optimising the steps and writing the paper. M.J.R., B.P., S.R.G., P.D., G.B. and L.K.I. tested the
600 software and assisted with the data analysis. S.K.G., R.D.H. and A.L.K.H. curated data. All the
601 authors reviewed the manuscript and provided detailed feedback. P.D., E.A.D. and R.A.E.
602 conceived the project and wrote the paper with input from all authors.

603 Acknowledgements

604 We thank Prof Christopher Quince for his insights and suggestions regarding the development
605 of methods. This research was undertaken with the resources and services from Flinders
606 University's High-Performance Computing platform ("Welcome to the DeepThought HPC —
607 DeepThought HPC Documentation" 2022).

608 Funding

609 This work is supported by the National Institutes of Health (NIH) National Institute of Diabetes
610 and Digestive and Kidney Diseases [RC2DK116713], the Australian Research Council
611 [DP220102915], and the Polish National Agency for Academic Exchange (NAWA) Bekker
612 Programme [BPN/BEK/2021/1/00416 to P.D.].

613 Conflict of Interest

614 None declared.

615 References

616 Albertsen, Mads, Philip Hugenholtz, Adam Skarszewski, Kåre L. Nielsen, Gene W. Tyson, and
617 Per H. Nielsen. 2013. "Genome Sequences of Rare, Uncultured Bacteria Obtained by
618 Differential Coverage Binning of Multiple Metagenomes." *Nature Biotechnology* 31 (6):
619 533–38.
620 Amgarten, Deyvid, Lucas P. P. Braga, Aline M. da Silva, and João C. Setubal. 2018. "MARVEL,
621 a Tool for Prediction of Bacteriophage Sequences in Metagenomic Bins." *Frontiers in*

622 *Genetics*. <https://doi.org/10.3389/fgene.2018.00304>.

623 Auslander, Noam, Ayal B. Gussow, Sean Benler, Yuri I. Wolf, and Eugene V. Koonin. 2020.

624 “Seeker: Alignment-Free Identification of Bacteriophage Genomes by Deep Learning.”

625 *Nucleic Acids Research* 48 (21): e121.

626 Baijens, Jasmijn A., Leen Stougie, and Alexander Schönthuth. 2020. “Strain-Aware Assembly

627 of Genomes from Mixed Samples Using Flow Variation Graphs.”

628 <https://doi.org/10.1101/645721>.

629 Bankevich, Anton, Sergey Nurk, Dmitry Antipov, Alexey A. Gurevich, Mikhail Dvorkin, Alexander

630 S. Kulikov, Valery M. Lesin, et al. 2012. “SPAdes: A New Genome Assembly Algorithm and

631 Its Applications to Single-Cell Sequencing.” *Journal of Computational Biology: A Journal of*

632 *Computational Molecular Cell Biology* 19 (5): 455–77.

633 Belcaid, Mahdi, Anne Bergeron, and Guylaine Poisson. 2010. “Mosaic Graphs and Comparative

634 Genomics in Phage Communities.” *Journal of Computational Biology: A Journal of*

635 *Computational Molecular Cell Biology* 17 (9): 1315–26.

636 Breitbart, Mya, Peter Salamon, Bjarne Andresen, Joseph M. Mahaffy, Anca M. Segall, David

637 Mead, Farooq Azam, and Forest Rohwer. 2002. “Genomic Analysis of Uncultured Marine

638 Viral Communities.” *Proceedings of the National Academy of Sciences of the United States*

639 *of America* 99 (22): 14250–55.

640 Casjens, Sherwood R., and Eddie B. Gilcrease. 2009. “Determining DNA Packaging Strategy by

641 Analysis of the Termini of the Chromosomes in Tailed-Bacteriophage Virions.” *Methods in*

642 *Molecular Biology* 502: 91–111.

643 Chen, Jiao, Yingchao Zhao, and Yanni Sun. 2018. “De Novo Haplotype Reconstruction in Viral

644 Quasispecies Using Paired-End Read Guided Path Finding.” *Bioinformatics* 34 (17): 2927–

645 35.

646 Chen, Lin-Xing, Karthik Anantharaman, Alon Shaiber, A. Murat Eren, and Jillian F. Banfield.

647 2020. “Accurate and Complete Genomes from Metagenomes.” *Genome Research* 30 (3):

648 315–33.

649 Comeau, André M., Graham F. Hatfull, Henry M. Krisch, Debbie Lindell, Nicholas H. Mann, and

650 David Prangishvili. 2008. “Exploring the Prokaryotic Virosphere.” *Research in Microbiology*

651 159 (5): 306–13.

652 Cook, Ryan, Nathan Brown, Tamsin Redgwell, Branko Rihtman, Megan Barnes, Martha Clokie,

653 Dov J. Stekel, Jon Hobman, Michael A. Jones, and Andrew Millard. 2021. “INfrastructure

654 for a PHAge REference Database: Identification of Large-Scale Biases in the Current

655 Collection of Cultured Phage Genomes.” *PHAGE (New Rochelle, N.Y.)* 2 (4): 214–23.

656 Delgado, Luis Fernando, and Anders F. Andersson. 2022. “Evaluating Metagenomic Assembly

657 Approaches for Biome-Specific Gene Catalogues.” *Microbiome* 10 (1): 72.

658 Dias, Fernando H. C., Lucia Williams, Brendan Mumey, and Alexandru I. Tomescu. 2022.

659 “Efficient Minimum Flow Decomposition via Integer Linear Programming.” *Journal of*

660 *Computational Biology: A Journal of Computational Molecular Cell Biology* 29 (11): 1252–

661 67.

662 Domingo, Esteban, and Celia Perales. 2019. “Viral Quasispecies.” *PLoS Genetics* 15 (10):

663 e1008271.

664 Dupont, Chris L., Douglas B. Rusch, Shibu Yooseph, Mary-Jane Lombardo, R. Alexander

665 Richter, Ruben Valas, Mark Novotny, et al. 2012. “Genomic Insights to SAR86, an

666 Abundant and Uncultivated Marine Bacterial Lineage.” *The ISME Journal* 6 (6): 1186–99.

667 Eddy, Sean R. 2011. “Accelerated Profile HMM Searches.” *PLoS Computational Biology* 7 (10):

668 e1002195.

669 Edwards, Robert A., and Forest Rohwer. 2005. “Viral Metagenomics.” *Nature Reviews*

670 *Microbiology* 3 (6): 504–10.

671 Freire, Borja, Susana Ladra, Jose R. Paramá, and Leena Salmela. 2021. “Inference of Viral

672 Quasispecies with a Paired de Bruijn Graph.” *Bioinformatics*.

673 https://doi.org/10.1093/bioinformatics/btaa782.
674 Freire, Borja, Susana Ladra, Jose R. Parama, and Leena Salmela. 2022. "ViQUF: De Novo
675 Viral Quasispecies Reconstruction Using Unitig-Based Flow Networks." *IEEE/ACM
676 Transactions on Computational Biology and Bioinformatics / IEEE, ACM PP* (July).
677 https://doi.org/10.1109/TCBB.2022.3190282.
678 Gatter, Thomas, and Peter F. Stadler. 2019. "Ryūtō: Network-Flow Based Transcriptome
679 Reconstruction." *BMC Bioinformatics* 20 (1): 190.
680 Gourlé, Hadrien, Oskar Karlsson-Lindsjö, Juliette Hayer, and Erik Bongcam-Rudloff. 2019.
681 "Simulating Illumina Metagenomic Data with InSilicoSeq." *Bioinformatics* 35 (3): 521–22.
682 Gunasekera, Samantha, Sam Abraham, Marc Stegger, Stanley Pang, Penghao Wang, Shafi
683 Sahibzada, and Mark O'Dea. 2021. "Evaluating Coverage Bias in next-Generation
684 Sequencing of *Escherichia Coli*." *PLoS One* 16 (6): e0253440.
685 Hatfull, Graham F. 2008. "Bacteriophage Genomics." *Current Opinion in Microbiology* 11 (5):
686 447–53.
687 Hesse, Ryan D., Michael Roach, Emma N. Kerr, Bhavya Papudeshi, Laís F. O. Lima, Asha Z.
688 Goodman, Lisa Hoopes, et al. 2022. "Phage Diving: An Exploration of the Carcharhinid
689 Shark Epidermal Virome." *Viruses* 14 (9). https://doi.org/10.3390/v14091969.
690 Hugenholtz, P., B. M. Goebel, and N. R. Pace. 1998. "Impact of Culture-Independent Studies on
691 the Emerging Phylogenetic View of Bacterial Diversity." *Journal of Bacteriology* 180 (18):
692 4765–74.
693 Johansen, Joachim, Damian R. Plichta, Jakob Nybo Nissen, Marie Louise Jespersen, Shiraz A.
694 Shah, Ling Deng, Jakob Stokholm, et al. 2022. "Genome Binning of Viral Entities from Bulk
695 Metagenomics Data." *Nature Communications* 13 (1): 965.
696 Jurtz, Vanessa Isabell, Julia Villarroel, Ole Lund, Mette Voldby Larsen, and Morten Nielsen.
697 2016. "MetaPhinder—Identifying Bacteriophage Sequences in Metagenomic Data Sets."
698 *PLOS ONE*. https://doi.org/10.1371/journal.pone.0163111.
699 Kang, Dongwan D., Feng Li, Edward Kirton, Ashleigh Thomas, Rob Egan, Hong An, and Zhong
700 Wang. 2019. "MetaBAT 2: An Adaptive Binning Algorithm for Robust and Efficient Genome
701 Reconstruction from Metagenome Assemblies." *PeerJ* 7 (July): e7359.
702 Kececioglu, J. D., and E. W. Myers. 1995. "Combinatorial Algorithms for DNA Sequence
703 Assembly." *Algorithmica*. https://doi.org/10.1007/bf01188580.
704 Keen, Eric C. 2015. "A Century of Phage Research: Bacteriophages and the Shaping of Modern
705 Biology." *BioEssays: News and Reviews in Molecular, Cellular and Developmental Biology*
706 37 (1): 6–9.
707 Kieft, Kristopher, Zhichao Zhou, and Karthik Anantharaman. 2020. "VIBRANT: Automated
708 Recovery, Annotation and Curation of Microbial Viruses, and Evaluation of Viral Community
709 Function from Genomic Sequences." *Microbiome* 8 (1): 90.
710 Kolmogorov, Mikhail, Jeffrey Yuan, Yu Lin, and Pavel A. Pevzner. 2019. "Assembly of Long,
711 Error-Prone Reads Using Repeat Graphs." *Nature Biotechnology* 37 (5): 540–46.
712 Lamurias, Andre, Mantas Sereika, Mads Albertsen, Katja Hose, and Thomas Dyrre Nielsen.
713 2022. "Metagenomic Binning with Assembly Graph Embeddings." *Bioinformatics* 38 (19):
714 4481–87.
715 Li, Dinghua, Chi-Man Liu, Ruibang Luo, Kunihiko Sadakane, and Tak-Wah Lam. 2015.
716 "MEGAHIT: An Ultra-Fast Single-Node Solution for Large and Complex Metagenomics
717 Assembly via Succinct de Bruijn Graph." *Bioinformatics*.
718 https://doi.org/10.1093/bioinformatics/btv033.
719 Li, Heng. 2018. "Minimap2: Pairwise Alignment for Nucleotide Sequences." *Bioinformatics* 34
720 (18): 3094–3100.
721 Li, Heng, Bob Handsaker, Alec Wysoker, Tim Fennell, Jue Ruan, Nils Homer, Gabor Marth,
722 Goncalo Abecasis, Richard Durbin, and 1000 Genome Project Data Processing Subgroup.
723 2009. "The Sequence Alignment/Map Format and SAMtools." *Bioinformatics* 25 (16):

724 2078–79.

725 Lima-Mendez, Gipsi, Ariane Toussaint, and Raphael Leplae. 2011. “A Modular View of the
726 Bacteriophage Genomic Space: Identification of Host and Lifestyle Marker Modules.”
727 *Research in Microbiology* 162 (8): 737–46.

728 Luque, Antoni, Sean Benler, Diana Y. Lee, Colin Brown, and Simon White. 2020. “The Missing
729 Tailed Phages: Prediction of Small Capsid Candidates.” *Microorganisms* 8 (12): 1944.

730 Łusiak-Szelachowska, Marzanna, Beata Weber-Dąbrowska, Ewa Jończyk-Matysiak, Renata
731 Wojciechowska, and Andrzej Górska. 2017. “Bacteriophages in the Gastrointestinal Tract
732 and Their Implications.” *Gut Pathogens* 9 (August): 44.

733 Mallawaarachchi, Vijini G., Anuradha S. Wickramarachchi, and Yu Lin. 2020. “GraphBin2:
734 Refined and Overlapped Binning of Metagenomic Contigs Using Assembly Graphs.” In *20th
735 International Workshop on Algorithms in Bioinformatics (WABI 2020)*, 21. Schloss Dagstuhl
736 - Leibniz-Zentrum für Informatik.

737 ———. 2021. “Improving Metagenomic Binning Results with Overlapped Bins Using Assembly
738 Graphs.” *Algorithms for Molecular Biology: AMB* 16 (1): 3.

739 Mallawaarachchi, Vijini, and Yu Lin. 2022a. “MetaCoAG: Binning Metagenomic Contigs via
740 Composition, Coverage and Assembly Graphs.” *Research in Computational Molecular
741 Biology: ... Annual International Conference, RECOMB: Proceedings. International
742 Conference on Research in Computational Molecular Biology*, 70–85.

743 ———. 2022b. “Accurate Binning of Metagenomic Contigs Using Composition, Coverage, and
744 Assembly Graphs.” *Journal of Computational Biology: A Journal of Computational
745 Molecular Cell Biology* 29 (12): 1357–76.

746 Mallawaarachchi, Vijini, Anuradha Wickramarachchi, and Yu Lin. 2020. “GraphBin: Refined
747 Binning of Metagenomic Contigs Using Assembly Graphs.” *Bioinformatics* 36 (11): 3307–
748 13.

749 Marçais, Guillaume, Arthur L. Delcher, Adam M. Phillippy, Rachel Coston, Steven L. Salzberg,
750 and Aleksey Zimin. 2018. “MUMmer4: A Fast and Versatile Genome Alignment System.”
751 *PLoS Computational Biology* 14 (1): e1005944.

752 McNair, Katelyn, Barbara A. Bailey, and Robert A. Edwards. 2012. “PHACTS, a Computational
753 Approach to Classifying the Lifestyle of Phages.” *Bioinformatics* 28 (5): 614–18.

754 Merrill, Bryan D., Andy T. Ward, Julianne H. Grose, and Sandra Hope. 2016. “Software-Based
755 Analysis of Bacteriophage Genomes, Physical Ends, and Packaging Strategies.” *BMC
756 Genomics* 17 (1): 679.

757 Meyer, Fernando, Adrian Fritz, Zhi-Luo Deng, David Koslicki, Till Robin Lesker, Alexey
758 Gurevich, Gary Robertson, et al. 2022. “Critical Assessment of Metagenome Interpretation:
759 The Second Round of Challenges.” *Nature Methods* 19 (4): 429–40.

760 Mikheenko, Alla, Vladislav Saveliev, and Alexey Gurevich. 2016. “MetaQUAST: Evaluation of
761 Metagenome Assemblies.” *Bioinformatics* 32 (7): 1088–90.

762 Namiki, Toshiaki, Tsuyoshi Hachiya, Hideaki Tanaka, and Yasubumi Sakakibara. 2012.
763 “MetaVelvet: An Extension of Velvet Assembler to de Novo Metagenome Assembly from
764 Short Sequence Reads.” *Nucleic Acids Research* 40 (20): e155.

765 Nayfach, Stephen, Antonio Pedro Camargo, Frederik Schulz, Emiley Eloe-Fadrosh, Simon
766 Roux, and Nikos C. Kyrpides. 2021. “CheckV Assesses the Quality and Completeness of
767 Metagenome-Assembled Viral Genomes.” *Nature Biotechnology* 39 (5): 578–85.

768 Nayfach, Stephen, David Páez-Espino, Lee Call, Soo Jen Low, Hila Sberro, Natalia N. Ivanova,
769 Amy D. Proal, et al. 2021. “Metagenomic Compendium of 189,680 DNA Viruses from the
770 Human Gut Microbiome.” *Nature Microbiology* 6 (7): 960–70.

771 Nissen, Jakob Nybo, Joachim Johansen, Rosa Lundbye Allesøe, Casper Kaae Sønderby, Jose
772 Juan Almagro Armenteros, Christopher Heje Grønbech, Lars Juhl Jensen, et al. 2021.
773 “Improved Metagenome Binning and Assembly Using Deep Variational Autoencoders.”
774 *Nature Biotechnology* 39 (5): 555–60.

775 Norman, Jason M., Scott A. Handley, Megan T. Baldridge, Lindsay Droit, Catherine Y. Liu, Brian
776 C. Keller, Amal Kambal, et al. 2015. "Disease-Specific Alterations in the Enteric Virome in
777 Inflammatory Bowel Disease." *Cell* 160 (3): 447–60.

778 Nurk, Sergey, Dmitry Meleshko, Anton Korobeynikov, and Pavel A. Pevzner. 2017.
779 "metaSPAdes: A New Versatile Metagenomic Assembler." *Genome Research* 27 (5): 824–
780 34.

781 Peng, Yu, Henry C. M. Leung, S. M. Yiu, and Francis Y. L. Chin. 2011. "Meta-IDBA: A de Novo
782 Assembler for Metagenomic Data." *Bioinformatics* 27 (13): i94–101.
783 ———. 2012. "IDBA-UD: A de Novo Assembler for Single-Cell and Metagenomic Sequencing
784 Data with Highly Uneven Depth." *Bioinformatics*.
785 <https://doi.org/10.1093/bioinformatics/bts174>.

786 Pevzner, P. A., H. Tang, and M. S. Waterman. 2001. "An Eulerian Path Approach to DNA
787 Fragment Assembly." *Proceedings of the National Academy of Sciences of the United
788 States of America* 98 (17): 9748–53.

789 Pevzner, Pavel A., Haixu Tang, and Glenn Tesler. 2004. "De Novo Repeat Classification and
790 Fragment Assembly." *Genome Research* 14 (9): 1786–96.

791 Pfeifer, Eugen, Rémy A. Bonnin, and Eduardo P. C. Rocha. 2022. "Phage-Plasmids Spread
792 Antibiotic Resistance Genes through Infection and Lysogenic Conversion." *mBio* 13 (5):
793 e0185122.

794 Pfeifer, Eugen, Jorge A. Moura de Sousa, Marie Touchon, and Eduardo P. C. Rocha. 2021.
795 "Bacteria Have Numerous Distinctive Groups of Phage-Plasmids with Conserved Phage
796 and Variable Plasmid Gene Repertoires." *Nucleic Acids Research* 49 (5): 2655–73.

797 Pritchard, Leighton, Rachel H. Glover, Sonia Humphris, John G. Elphinstone, and Ian K. Toth.
798 2015. "Genomics and Taxonomy in Diagnostics for Food Security: Soft-Rotting
799 Enterobacterial Plant Pathogens." *Analytical Methods* 8 (1): 12–24.

800 Quince, Christopher, Sergey Nurk, Sébastien Raguideau, Robert James, Orkun S. Soyer, J.
801 Kimberly Summers, Antoine Limasset, A. Murat Eren, Rayan Chikhi, and Aaron E. Darling.
802 2021. "STRONG: Metagenomics Strain Resolution on Assembly Graphs." *Genome Biology*
803 22 (1): 214.

804 Ravin, Nikolai V., Alexander N. Svarchevsky, and Gianni Dehò. 1999. "The Anti-Immunity
805 System of Phage-Plasmid N15: Identification of the Antirepressor Gene and Its Control by a
806 Small Processed RNA." *Molecular Microbiology* 34 (5): 980–94.

807 Rho, Mina, Haixu Tang, and Yuzhen Ye. 2010. "FragGeneScan: Predicting Genes in Short and
808 Error-Prone Reads." *Nucleic Acids Research*. <https://doi.org/10.1093/nar/gkq747>.

809 Roach, Michael J., Sarah J. Beecroft, Kathie A. Mihindukulasuriya, Leran Wang, Anne Paredes,
810 Kara Henry-Cocks, Lais Farias Oliveira Lima, Elizabeth A. Dinsdale, Robert A. Edwards,
811 and Scott A. Handley. 2022. "Hecatomb: An End-to-End Research Platform for Viral
812 Metagenomics." *bioRxiv*. <https://doi.org/10.1101/2022.05.15.492003>.

813 Roach, Michael J., Katelyn McNair, Maciej Michalczyk, Sarah K. Giles, Laura K. Inglis, Evan
814 Pargin, Jakub Barylski, Simon Roux, Przemysław Decewicz, and Robert A. Edwards. 2022.
815 "Philympics 2021: Prophage Predictions Perplex Programs." *F1000Research* 10 (758): 758.

816 Roach, Michael, Nuri Tessa Pierce-Ward, Radosław Sucecki, Vijini Mallawaarachchi, Bhavya
817 Papudeshi, Scott A. Handley, C. Titus Brown, Nathan S. Watson-Haigh, and Robert A.
818 Edwards. 2022. "Ten Simple Rules and a Template for Creating Workflows-as-
819 Applications." *PLoS Computational Biology* 8 (12): e1010705.

820 Rodriguez-Valera, Francisco, Ana-Belen Martin-Cuadrado, Beltran Rodriguez-Brito, Lejla Pasić,
821 T. Frede Thingstad, Forest Rohwer, and Alex Mira. 2009. "Explaining Microbial Population
822 Genomics through Phage Predation." *Nature Reviews Microbiology* 7 (11): 828–36.

823 Roux, Simon, Joanne B. Emerson, Emiley A. Eloe-Fadrosh, and Matthew B. Sullivan. 2017.
824 "Benchmarking Viromics: An in Silico Evaluation of Metagenome-Enabled Estimates of
825 Viral Community Composition and Diversity." *PeerJ* 5 (September): e3817.

826 Sanger, F., G. M. Air, B. G. Barrell, N. L. Brown, A. R. Coulson, C. A. Fiddes, C. A. Hutchison,
827 P. M. Slocombe, and M. Smith. 1977. "Nucleotide Sequence of Bacteriophage Phi X174
828 DNA." *Nature* 265 (5596): 687–95.

829 Schrijver, Alexander. 1998. *Theory of Linear and Integer Programming*. John Wiley & Sons.

830 Shao, Mingfu, and Carl Kingsford. 2017. "Accurate Assembly of Transcripts through Phase-
831 Preserving Graph Decomposition." *Nature Biotechnology*. <https://doi.org/10.1038/nbt.4020>.

832 Shimoyama, Y. 2022. "pyGenomeViz." pyGenomeViz. 2022.
<https://moshi4.github.io/pyGenomeViz/>.

833 Simmonds, Peter, Mike J. Adams, Mária Benkő, Mya Breitbart, J. Rodney Brister, Eric B.
834 Carstens, Andrew J. Davison, et al. 2017. "Consensus Statement: Virus Taxonomy in the
835 Age of Metagenomics." *Nature Reviews. Microbiology* 15 (3): 161–68.

836 Steinegger, Martin, and Johannes Söding. 2017. "MMseqs2 Enables Sensitive Protein
837 Sequence Searching for the Analysis of Massive Data Sets." *Nature Biotechnology* 35 (11):
838 1026–28.

839 Sutton, Thomas D. S., Adam G. Clooney, Feargal J. Ryan, R. Paul Ross, and Colin Hill. 2019.
840 "Choice of Assembly Software Has a Critical Impact on Virome Characterisation."
841 *Microbiome* 7 (1): 1–15.

842 Terzian, Paul, Eric Olo Ndela, Clovis Galiez, Julien Lossouarn, Rubén Enrique Pérez Bucio,
843 Robin Mom, Ariane Toussaint, Marie-Agnès Petit, and François Enault. 2021. "PHROG:
844 Families of Prokaryotic Virus Proteins Clustered Using Remote Homology." *NAR Genomics
845 and Bioinformatics* 3 (3): Iqab067.

846 Tomescu, Alexandru I., Anna Kuosmanen, Romeo Rizzi, and Veli Mäkinen. 2013. "A Novel Min-
847 Cost Flow Method for Estimating Transcript Expression with RNA-Seq." *BMC
848 Bioinformatics* 14 Suppl 5 (Suppl 5): S15.

849 Twort, F. W. 1915. "AN INVESTIGATION ON THE NATURE OF ULTRA-MICROSCOPIC
850 VIRUSES." *The Lancet*. [https://doi.org/10.1016/s0140-6736\(01\)20383-3](https://doi.org/10.1016/s0140-6736(01)20383-3).

851 Vatinlen, B., F. Chauvet, P. Chrétienne, and P. Mahey. 2008. "Simple Bounds and Greedy
852 Algorithms for Decomposing a Flow into a Minimal Set of Paths." *European Journal of
853 Operational Research*. <https://doi.org/10.1016/j.ejor.2006.05.043>.

854 "Welcome to the DeepThought HPC — DeepThought HPC Documentation." 2022. 2022.
855 <https://doi.org/10.25957/FLINDERS.HPC.DEEPTHOUGHT>.

856 Wick, Ryan R., Mark B. Schultz, Justin Zobel, and Kathryn E. Holt. 2015. "Bandage: Interactive
857 Visualization of de Novo Genome Assemblies." *Bioinformatics* 31 (20): 3350–52.

858 Woodcroft, B. J., and R. Newell. 2017. "GitHub - wwood/CoverM: Read Coverage Calculator for
859 Metagenomics." GitHub. 2017. <https://github.com/wwood/CoverM>.

860 Xue, Hansheng, Vijini Mallawaarachchi, Yujia Zhang, Vaibhav Rajan, and Yu Lin. 2022.
861 "RepBin: Constraint-Based Graph Representation Learning for Metagenomic Binning."
862 *Proceedings of the AAAI Conference on Artificial Intelligence*.
863 <https://doi.org/10.1609/aaai.v36i4.20388>.

864 Yeon-Bo Chung et al. 1990. "Bacteriophage T7 DNA Packaging: III. A 'Hairpin' End Formed on
865 T7 Concatemers May Be an Intermediate in the Processing Reaction." *Journal of Molecular
866 Biology* 216 (4): 939–48.

867 Zhang, Xing, and F. William Studier. 2004. "Multiple Roles of T7 RNA Polymerase and T7
868 Lysozyme during Bacteriophage T7 Infection." *Journal of Molecular Biology* 340 (4): 707–
869 30.

870